

# Theoretical Analysis of Two Novel Hybrid Thermoelectric-Photovoltaic Systems Based on $\text{Cu}_2\text{ZnSnS}_4$ Solar Cells

Bruno Lorenzi<sup>1,\*</sup>, Gaetano Contento<sup>2</sup>, Vincenzo Sabatelli<sup>3</sup>, Antonella Rizzo<sup>2</sup>, and Dario Narducci<sup>1</sup>

<sup>1</sup>*Department of Material Science, University of Milano Bicocca, via R. Cozzi 55, 20125 Milano, Italy*

<sup>2</sup>*Ente per le Nuove Tecnologie l'Energia e l'Ambiente, Brindisi Research Centre, Department of Sustainable Territorial and Production Systems—Division of Materials Technologies and Processing for Sustainability, SS 7 Appia km 730, 72100 Brindisi, Italy*

<sup>3</sup>*ENEA Trisaia Research Centre, Department of Energy Technologies—Division of Solar Thermal and Thermodynamic, SS 106 Jonica km 419.5, 75026 Rotondella (MT)-Italy*

The development and commercialization of Photovoltaic (PV) cells with good cost-efficiency trade-off not using critical raw materials (CRMs) is one of the strategies chosen by the European Community (EC) to address the Energy Roadmap 2050. In this context  $\text{Cu}_2\text{ZnSnS}_4$  (CZTS) solar cells are attracting a major interest since they have the potential to combine low price with relatively high conversion efficiencies. Although a  $\approx 9\%$  lab scale efficiency has already been reported for CZTS this technology is still far from being competitive in terms of cost per peak-power ( $\text{€}/\text{W}_p$ ) with other common materials. One possible near-future solution to increase the CZTS competitiveness comes from thermoelectrics. Actually it has already been shown that Hybrid Thermoelectric-Photovoltaic Systems (HTEPVs) based on CIGS, another kesterite very similar to CZTS, can lead to a significant efficiency improvement. However it has been also clarified how the optimal hybridization strategy cannot come from the simple coupling of solar cells with commercial TEGs, but special layouts have to be implemented. Furthermore, since solar cell performances are well known to decrease with temperature, thermal decoupling strategies of the PV and TEG sections have to be taken. To address these issues, we developed a model for two different HTEPV solutions, both coupled with CZTS solar cells. In the first case we considered a Thermally-Coupled HTEPV device (TC-HTEPV) in which the TEG is placed underneath the solar cell and in thermal contact with it. The second system consists instead of an Optically-Coupled but thermally decoupled device (OC-HTEPV) in which part of the solar spectrum is focused by a non-imaging optical concentrator on the TEG hot side. For both solutions the model returns conversion efficiencies higher than that of the CZTS solar cell alone. Specifically, increases of  $\approx 30\%$  are predicted for both kind of systems considered.

**Keywords:** Hybrid Solar Cells, Thermoelectric Generators, Photovoltaic Cell, Solar Energy.

## 1. INTRODUCTION

The need for efficient renewable sources of energy, able to satisfy the continually increasing demand of electric power in the framework of a constant reduction of fossil fuels, is the key challenge for the twenty-first century. Solar energy is widely recognized as one of the best candidates to face this challenge in a near future perspective. For this reason the development and the commercialization of novel PV devices with good cost-effectiveness has

become a primary strategy in the policy of a great number of countries. Within the European Communities (EC) this trend has been joined with a focus towards technologies using non critical-raw materials (CRMs). Actually, in 2010 the European commission introduced a methodology to identify those materials, creating in 2011 a first list of 14 CRMs, revised to 20 in 2014.

In this context  $\text{Cu}_2\text{ZnSnS}$  (CZTS) single-junction solar cells are attracting a major interest since they have the potential to combine low price with the use of abundant and non-toxic elements and relatively high conversion

\*Author to whom correspondence should be addressed.

efficiencies. CZTS is a semiconductor alloy with a high absorption coefficient and a direct energy gap ( $E_g$ ) of  $\approx 1.5$  eV.<sup>1</sup> Recently the know-how on CIGS solar cells has been exploited to realize CZTS thin films for PV application. During the last five years a large number of physical and chemical deposition methods have been tested to this scope. This effort led in the 2013 to a record efficiency of 9.1%,<sup>2</sup> however obtained with the use of CdS as buffer layer. Since Cd-based materials are toxic, nowadays Cd-free buffer layers such as ZnS and ZnSe are preferred. Unfortunately Cd-free CZTS solar cells have been reported to achieve smaller efficiencies. Therefore CZTS is still far from being competitive with silicon and other common PV materials. Actually even though its cost effectiveness is very good compared to standard technologies, the available efficiencies are still bound to too small values. Thus in terms of cost per peak-power ( $\text{€}/W_p$ ) CZTS cannot nowadays compete yet.

One possible near-future solution to increase the CZTS competitiveness comes from thermoelectrics. Actually it has already been shown that a significant efficiency improvement can be achieved placing a commercial thermoelectric generator (TEG) in thermal contact with the back of a CIGS solar cell.<sup>3</sup> However the experimental procedures reported in literature for such Hybrid Thermoelectric-Photovoltaic Systems (HTEPVs) have been often affected by too optimistic settings of the cold sink temperature that may possibly have led to overestimate the HTEPV efficiency. In addition it has been also clarified how an optimized hybridization strategy cannot come from the simple coupling of solar cells with commercial TEGs.<sup>4</sup> Actually, special layouts have to be implemented to have the HTEPV device working at its optimum temperature. Finally, since solar cell performances are well known to decrease with temperature, thermal decoupling strategies of the PV and TEG sections should be implemented.

To better understand and address these issues, in this work we have developed a model for two different HTEPV solutions: a Thermally-Coupled device (TC-HTEPV), and an Optically-Coupled but thermally decoupled device (OC-HTEPV).

## 2. MODEL DESCRIPTION

In this section we will describe the scheme of the two HTEPV systems. We will present the model used for simulations and will justify the assumptions we made.

### 2.1. System Description

As already pointed out in a previous publication,<sup>5</sup> in a solar cell three main losses exist because of the mismatch between the solar spectrum and the absorber. The first, hereafter  $L_{2a}$ , comes from photons that cannot be absorbed because they have energies smaller than the  $E_g$  of the absorber material. The second, hereafter  $L_{2b}$ , comes from absorbed photons having energies larger than the  $E_g$  of the

absorber material. Actually these photons generate hot carriers that will then thermalize, leading to the heating of the solar cell. The third loss (which is a direct consequence of  $L_{2b}$ ) comes from the efficiency degradation due to cell heating. Actually it is well known that the higher is the device temperature, the higher is the carrier recombination rate, and thus the efficiency degradation.<sup>6</sup> We will call this latter loss  $L_{2c}$ , which is obviously dependent on the cell temperature ( $T_{PV}$ ). Details on these losses as a function of  $E_g$  are reported in a previous publication.<sup>5</sup>

As mentioned, some of the lost power can be recovered by coupling of solar cell with TEGs. Figure 1 shows the schemes of the two HTEPV devices considered in this work. In the OC-HTEPV system (Fig. 1(a))  $L_{2a}$  is focused on the TEG hot side by means of a non-imaging optical concentrator, namely a Compound Parabolic Concentrator (CPC). This type of non-imaging concentrator is in general comprised of two parabolic mirror segments that trap sun rays coming from any angle between the focal line and the acceptance angle, reflecting them above the receiver that can be a flat plate located at the base of the intersection of the two parabola.<sup>7,8</sup> In operation, the CPC is usually installed with its receiver axis aligned along E–W direction. The aperture of the CPC is typically tilted toward the South so that the incident solar irradiance enters within the acceptance angle of the CPC. If during the sun apparent motion the incident solar irradiance does not fall outside the CPC acceptance angle, no tracking of the CPC aperture is needed. However, the tilt of the CPC aperture may have to be adjusted periodically during the year if the incident solar irradiance moves outside the CPC acceptance angle. In the OC-HTEPV a transparent solar cell back-contact and a suitable Solar Selective Absorber (SSA) are needed. Note that in this system neither  $L_{2b}$  nor  $L_{2c}$  losses can be recovered. However the advantage of the thermal decoupling between the PV and TEG parts is expected to positively impact on  $L_{2c}$ , since  $T_{PV}$  is expected to remain relatively small. Furthermore, it may be worth noting that the principle of the thermal concentration as conceived by Kraemer and co-authors in the case of pure Solar Thermoelectric Generators (STEGs)<sup>9</sup> can be implemented to optimize the cell and the TEG working temperature.

In the TC-HTEPV system (Fig. 1(b)), instead, the TEG is placed underneath the solar cell, in thermal contact with it. In this case  $L_{2a}$  can be converted into heat by an opaque back contact with suitable optical characteristics. A common metallic back contact with reduced reflectance can be used to this purpose. Therefore in the TC-HTEPV system both  $L_{2a}$  and  $L_{2b}$  contribute to set the cell temperature and consequently the TEG hot side temperature. However no possibility to avoid the  $L_{2c}$  loss is conceivable. Also in this case thermal concentration can be used.

From an electrical point of view both devices are thought and modeled in a configuration for which the PV and the TEG parts are connected to two different electrical

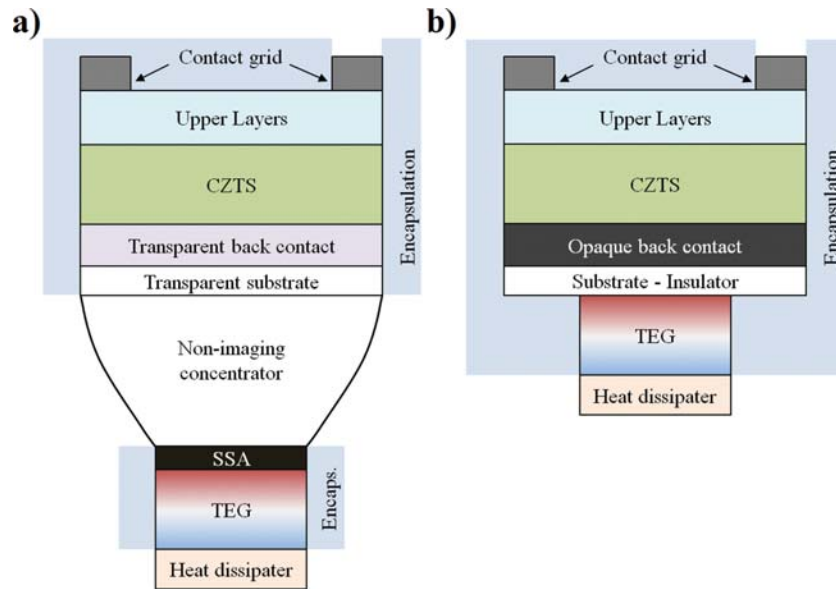


Figure 1. Schematics of (a) the OC-HTEPV system and (b) the TC-HTEPV system.

loads. Thus the HTEPV output power is simply the sum of the PV and TEG output powers:

$$P_{\text{HTEPV}} = P_{\text{PV}} + P_{\text{TEG}} \quad (1)$$

Thus the hybrid efficiency reads

$$\eta_{\text{HTEPV}} = \eta_{\text{PV}} + \eta_{\text{opt}} \eta_{\text{TEG}} \quad (2)$$

where  $\eta_{\text{PV}}$  and  $\eta_{\text{TEG}}$  are respectively the PV and TEG efficiencies, and  $\eta_{\text{opt}}$  is the system efficiency in converting the optical input power into heat flowing through the TEG, as shown by Chen.<sup>10</sup> Details for these efficiencies will be reported in Section 3.

The case of electrically hybridized HTEPV device can lead to different results<sup>11</sup> but will not be analyzed in this work.

## 2.2. Thermal Circuits

Figure 2 displays the thermal circuits for the two HTEPV systems. In this picture circles mark the main nodes of the systems, squares are the thermal resistances between nodes, and the arrows display the incoming power. For sake of clarity the circuits have been divided in three main sections.

In the OC-HTEPV case (Fig. 2(a)), there are two incoming power nodes. The first is at the PV section with an incoming power

$$P_{\text{in,PV}}^{\text{OC}} = [1 - L_{2a} - \eta_{\text{PV}}] \tau_{\text{enc}} S G \quad (3)$$

where  $\tau_{\text{enc}}$  is encapsulation transmittance,  $G$  the global solar irradiance on the aperture plane,  $\eta_{\text{PV}}$  the PV conversion efficiency, and  $S$  is the aperture area. The second node

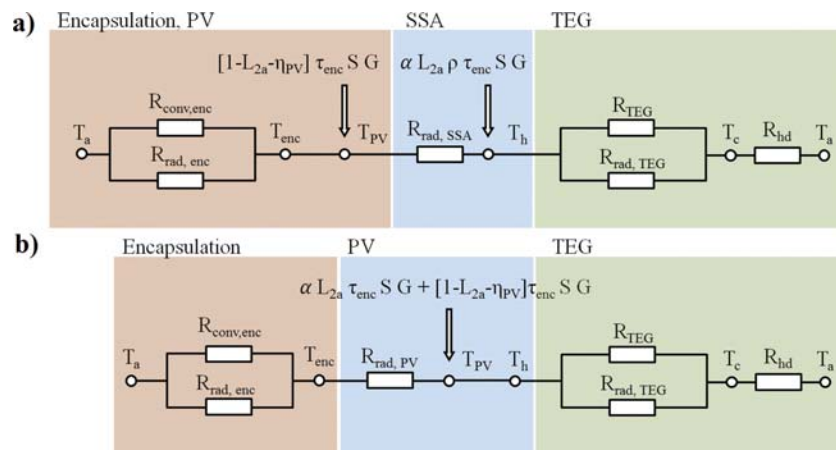


Figure 2. Thermal circuit for (a) the OC-HTEPV system and (b) the TC-HTEPV system.

is instead at the SSA section, with an incoming power given by

$$P_{in,SSA}^{OC} = \alpha L_{2a} \rho \tau_{enc} SG \quad (4)$$

with  $\alpha$  the SSA absorbance, and  $\rho$  the optical transmittance of CPC as set by the concentrator reflectance and the mean number of reflections.<sup>8</sup> To evaluate the thermal power flowing through the TEG, it has to be considered that only a fraction of the PV thermal power, hereafter called  $f$ , will be intercepted by the TEG, so that

$$P_{in,TEG}^{OC} = f P_{in,PV}^{OC} + P_{in,SSA}^{OC} \quad (5)$$

with  $f = R_{up}/(R_{down} + R_{up})$  and  $R_{up}$  and  $R_{down}$  are respectively the upper and lower thermal resistances. They can be written as

$$R_{up} = R_{rad,SSA} + \left( \frac{1}{1/R_{conv,enc} + 1/R_{rad,enc}} \right) \quad (6)$$

$$R_{down} = R_{hd} + \left( \frac{1}{1/R_{TEG} + 1/R_{rad,TEG}} \right) \quad (7)$$

where  $R_{rad,SSA}$ ,  $R_{rad,enc}$ , and  $R_{rad,TEG}$  are respectively the SSA, the encapsulation, and the TEG radiative thermal resistances;  $R_{conv,enc}$  and  $R_{hd}$  are the encapsulation and heat dissipater convective thermal resistances; while  $R_{TEG}$  is the TEG thermal resistance.

Another fact to consider is that, since optical concentration is used, it is necessary to distinguish between the PV area  $S$  and the TEG area  $A$ , which are related to each other as

$$C_{opt} = \frac{S}{A} \quad (8)$$

whit  $C_{opt}$  the geometric concentration ratio.

The unknown parameters for the OC-HTEPV system are  $T_{PV}$ ,  $T_h$ , and  $T_c$ , which are respectively the PV, the TEG hot and cold side temperatures. For this system we may assume that  $T_{PV} = T_{enc}$ . Regarding instead the TC-HTEPV system (Fig. 2(b)), there is only one incoming power node at the PV section, with

$$P_{in,TEG}^{TC} = \alpha L_{2a} \tau_{enc} SG + [(1 - L_{2a}) - \eta_{PV}] \tau_{enc} SG \quad (9)$$

where  $\alpha$  is the absorbance of back contact, which for simplicity will be taken equal to the SSA absorbance. The first term represents the incoming solar power transmitted through the active layer of solar cell and absorbed by the back contact, whereas the second is the fraction of the incoming solar power lost as heat in the PV section.

The unknown variables of the circuit are  $T_{enc}$ ,  $T_{PV}$  and  $T_c$ , with  $T_{enc}$  the encapsulation temperature. Actually, since the TEG is in thermal contact with the solar cell, for simplicity we may assume that

$$T_{PV} = T_h$$

From a comparison between the two thermal circuits, it is clear how the TC-HTEPV can be considered as a special

case of the OC-HTEPV. Actually, assuming that the back contact and the SSA have the same absorbance, that the two system have the same enclosure, and that the TC-HTEPV system has no optical concentration, Eq. (9) is a limiting case of Eq. (5) with  $\rho = f = C_{opt} = 1$ .

### 2.3. Model Equations

The main equations used to solve the thermal circuits described above follow. Thermal resistances of Figure 2 can be written as:

$$\frac{1}{R_{conv,enc}} = S h_{conv} \quad (10)$$

where  $h_{conv}$  is the convective coefficient of the encapsulation top surface.

$$\frac{1}{R_{rad,enc}} = S \sigma \varepsilon_{enc,ext} (T_{enc}^2 + T_a^2) (T_{enc} + T_a) \quad (11)$$

where  $\sigma$  is the Stefan-Boltzmann constant and  $\varepsilon_{enc,ext}$  the external exposed encapsulation emissivity; and

$$\frac{1}{R_{rad,PV}} = \frac{1}{R_{rad,SSA}} = A \sigma \varepsilon_{ABS,enc} (T_h^2 + T_{enc}^2) (T_h + T_{enc}) \quad (12)$$

where  $\varepsilon_{ABS,enc}$  is the equivalent emissivity for the case of an absorber of area  $A$  (the SSA for the OC-HTEPV device) facing the internal face of the front enclosure with aperture area  $S$ . This equivalent emissivity can be approximated as (cf. Appendix):

$$\varepsilon_{ABS,enc} = \left( \frac{1 - \varepsilon_h}{\varepsilon_h} + 1 + \frac{1 - \varepsilon_{enc,int}}{C_{opt} \varepsilon_{enc,int}} \right)^{-1} \quad (13)$$

where we assumed a view factor between absorber and aperture equal to one for the OC, and where  $\varepsilon_h$  and  $\varepsilon_{enc,int}$  are the emissivity of the upper surface of the absorber, and of the encapsulation internal surface. However, the same expression can be used also for the PV cell in the TC-HTEPV device, as such expression is properly reduced to that of two large, (infinite) facing surfaces of equal area when  $A = S$  and  $C_{opt} = 1$  (cf. Appendix).

Concerning  $R_{rad,TEG}$  it may be written assuming that the system operates under vacuum and with the metal interconnections (MI) within the TEG placed in front of each other (Fig. 1) onto two very large (infinite) parallel surfaces (cf. Appendix). Thus

$$\frac{1}{R_{rad,TEG}} = A \sigma \varepsilon_{TEG} (T_h^2 + T_c^2) (T_h + T_c) \quad (14)$$

where  $\varepsilon_{TEG}$  is the TEG equivalent emissivity.

Also

$$\varepsilon_{TEG} = \left( \frac{1}{\varepsilon_{MI}} + \frac{1}{\varepsilon_{MI}} - 1 \right)^{-1} \quad (15)$$

Finally

$$\frac{1}{R_{hd}} = AU \quad (16)$$

where  $U$  is the dissipater convective heat-loss coefficient; and

$$\frac{1}{R_{\text{TEG}}} = \frac{k_n A_n}{L} + \frac{k_p A_p}{L} \quad (17)$$

with  $A_n$  and  $A_p$  the leg areas,  $L$  the leg length, and  $k_n$  and  $k_p$  their thermal conductivities. The geometrical ratios of TEG legs  $L/\sqrt{A_n}$  were purposely set to 1.22 as in Ref. [9] that was taken as our benchmark case.

In particular, the following relation holds between the area of TEG legs,  $A_n$  and  $A_p$  and the area of the PV module,  $S$ ,

$$C_{\text{th}} = \frac{S}{A_n + A_p} \quad (18)$$

where  $C_{\text{th}}$ , is the thermal concentration.

Once all thermo-physical and geometrical parameters ( $C_{\text{th}}$ ,  $C_{\text{opt}}$ ) and the ambient temperature  $T_a$  are set,  $T_h$ ,  $T_c$ ,  $T_{\text{enc}}$  can be found by solving the following set of equations:

$$Q(T_h, T_c) = -\frac{R}{2}I^2 + \frac{(T_h - T_c)}{R_{\text{TEG}}} + S_{pn}IT_h \quad (19)$$

$$P_{\text{in,TEG}}^{\text{OC}} = P_{\text{in,TEG}}^{\text{TC}} = Q(T_h, T_c) + \frac{(T_h - T_{\text{enc}})}{R_{\text{rad,SSA}}} + \frac{(T_h - T_c)}{R_{\text{rad,TEG}}} \quad (20)$$

$$\frac{(T_{\text{enc}} - T_a)}{R_{\text{conv,enc}}} + \frac{(T_{\text{enc}} - T_a)}{R_{\text{rad,enc}}} = (1-f)P_{\text{in,PV}}^{\text{OC}} + \frac{(T_h - T_{\text{enc}})}{R_{\text{rad,SSA}}} \quad (21)$$

$$\frac{(T_c - T_a)}{R_{\text{hd}}} = \frac{R}{2}I^2 + \frac{(T_h - T_c)}{R_{\text{TEG}}} + S_{pn}IT_c \quad (22)$$

Assuming  $A_n = A_p$ , we obtain

$$I(T_h, T_c, C_{\text{tot}}) = \frac{S_{pn}(T_h - T_c)}{R(1 + \sqrt{1 + Z(T_h + T_c)/2})} \quad (23)$$

where

$$C_{\text{tot}} = C_{\text{th}}C_{\text{opt}} = \frac{A}{2A_n} \frac{S}{A} = \frac{S}{2A_n} \quad (24)$$

while

$$R = \frac{A_n}{\sigma_n L} + \frac{A_p}{\sigma_p L} = \frac{S}{2LC_{\text{tot}}} \left( \frac{1}{\sigma_n} + \frac{1}{\sigma_p} \right) \quad (25)$$

and

$$Z = \frac{S_{pn}^2}{(\sqrt{k_n/\sigma_n} + \sqrt{k_p/\sigma_p})^2} \quad (26)$$

with  $S_{pn}$  the Seebeck coefficient of a  $p$ - $n$  semiconductor couple,  $\sigma_n$ ,  $\sigma_p$  their electrical conductivities, and  $I$  the current flowing within the TEG legs.

### 3. PV AND TEG EFFICIENCIES

Manifestly enough, the HTEPV device efficiencies depend on the PV and TEG efficiencies. For the TEG, efficiency depends on the figure of merit  $ZT$  of the thermoelectric material used, and on  $T_h$  and  $T_c$ , as

$$\eta_{\text{TEG}} = \frac{\Delta T}{T_h} \frac{\sqrt{1 + Z\bar{T}} - 1}{\sqrt{1 + Z\bar{T}} + T_c/T_h} \quad (27)$$

with  $\Delta T = T_h - T_c$  and  $\bar{T} = (T_h + T_c)/2$ .

It should be noted that this is not the efficiency referred to the total external solar power harvested. Actually, one also needs to account for an optical efficiency, which is the system efficiency in converting the optical input power into heat flowing through the TEG as reported by Kraemer et al.<sup>9</sup>

$$\eta_{\text{opt}} = \frac{P_{\text{in,TEG}}^{\text{OC}} - [(T_h - T_{\text{enc}})/R_{\text{rad,SSA}} + (T_h - T_c)/R_{\text{rad,TEG}}]}{SG} \\ = \frac{Q(T_h, T_c)}{SG} \quad (28)$$

where  $P_{\text{in,TEG}}^{\text{OC}}$  can be replaced by  $P_{\text{in,TEG}}^{\text{TC}}$  to compute  $\eta_{\text{opt}}$  for the TC-HTEPV case.

Regarding instead the PV part we calculate the PV efficiency as function of the temperature as

$$\eta_{\text{PV}} = \eta_{\text{PV}}^0 [1 - \gamma(T_{\text{PV}} - T_{\text{SC}})] \quad (29)$$

where  $\eta_{\text{PV}}^0$  is the PV efficiency at Standard Condition temperature  $T_{\text{SC}} = 300$  K, and  $\gamma$  is its temperature coefficient. In this work we take  $\eta_{\text{PV}}^0 = 9.1\%$ <sup>12</sup> and  $\gamma = 0.0017 \text{ K}^{-1}$ .<sup>13</sup>

Finally, once the unknown temperatures are obtained, Eq. (2) can be used to obtain the HTEPV efficiency.

### 4. RESULTS AND DISCUSSION

The values used for the simulations carried out in this work are summarized in Table I. Thermoelectric properties of the TEG material were inherited from Kraemer et al.<sup>9</sup>

Note that the optical concentration has direct influence on the area of the thermoelectric device that needs to be covered with the heatsink having the desired heat-loss coefficient,  $U$ . For  $h_{\text{conv}}$  a value of  $10 \text{ W/m}^2\text{K}$  typical of free convection has been used.<sup>14,15</sup>

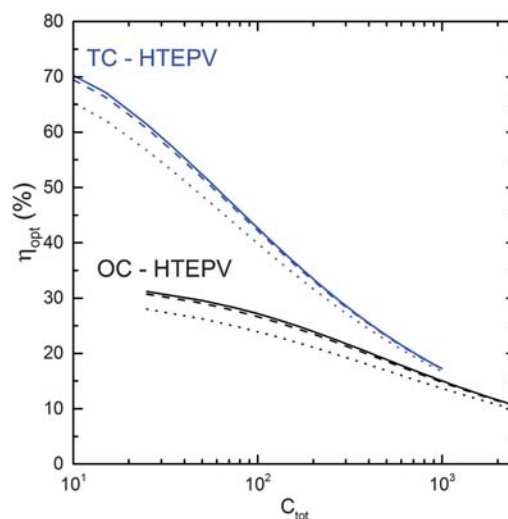
The left part of Figure 3 shows the total efficiencies of the two HTEPV systems versus the total concentration  $C_{\text{tot}}$ . In both cases three values of the dissipater heat-loss coefficient  $U$  were considered. For the TC-HTEPV, since  $C_{\text{opt}} = 1$ , only thermal concentration is taken into account, so that  $C_{\text{th}} = C_{\text{tot}}$ . For the OC-HTEPV system instead we reported the case of  $C_{\text{opt}} = 4$ , for which only seasonal tracking adjustments are needed.

One may note that the maximum efficiencies for the two systems are found for very different  $C_{\text{tot}}$  values. Actually while for the TC-HTEPV system the optimal  $C_{\text{tot}}$  is around 15, for the OC-HTEPV system it is more than one order of magnitude higher ( $C_{\text{tot}} \approx 200$ ). This means, considering that for the OC system the TEG area  $A$  is four times smaller than in the TC case, that the filling factor for the OC-HTEPV system should be more than three times smaller than in the TC-HTEPV case. This is mainly due to the fact that the TC-HTEPV device performs better at lower temperatures ( $\approx 475$  K) compared to the OC-HTEPV device ( $\approx 550$  K) as shown in the right part of Figure 3, where the total efficiencies of the two HTEPV systems are reported versus  $T_h$ . For the TC case in fact, the decrease of

**Table I.** Values of the parameters used in the simulations.

Description	Symbol	Value
Enclosure (glass) transmittance	$\tau$	0.94
Solar absorbance of SSA in OC-HTPEV $\equiv$ Solar absorbance of back contact in TC-HTPEV	$\alpha$	0.95
CPC transmittance	$\rho$	0.95 1 (Only for the TC case)
Sub-bandgap fraction of solar power	$L_{2a}$	0.40 (CZTS)
IR emissivity of SSA	$\varepsilon_h$	0.05
IR emissivity of external face of enclosure (glass)	$\varepsilon_{enc, ext}$	0.90
IR emissivity of internal face of enclosure (TC model) or PV substrate (OC model)	$\varepsilon_{enc, int}$	0.05
IR emissivity of faced and internal faces of TEG (copper)	$\varepsilon_{MI}$	0.07
Enclosure convective heat loss coefficient	$h_{conv}$	10 (W/m <sup>2</sup> K)
Global solar irradiance on the aperture area	$G$	1000 (W/m <sup>2</sup> )
Ambient temperature	$T_a$	25 (°C)
Seebeck coefficient	$S_{pn}$	$450 \times 10^{-6}$ (V/K)
Electrical conductivity	$\sigma_p \approx \sigma_n$	$6 \times 10^4$ (S/m)
Thermal conductivity	$k_p \approx k_n$	1 (W/mK)
Fraction of heat from PV incoming in TEG device	$f$	1 (Only for the TC-HTPEV)
Aperture area	$S$	0.018 (m <sup>2</sup> )

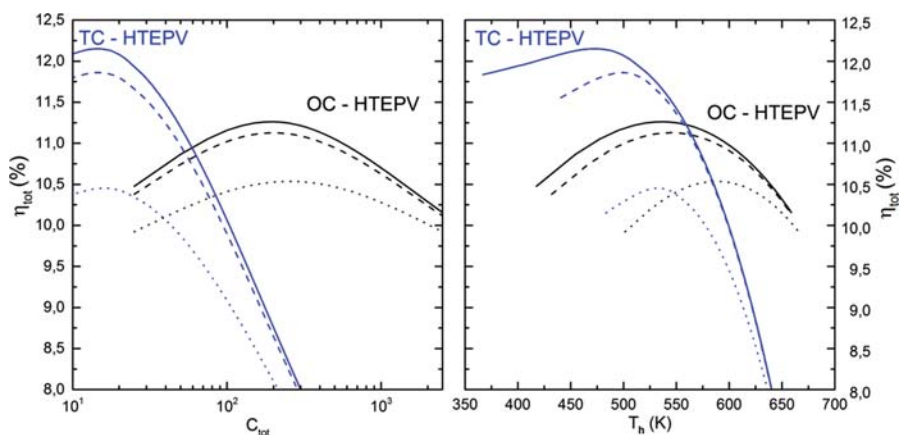
$\eta_{PV}$  is too large to be compensated by the TEG efficiency for temperature higher than 500 K. From Figure 3 (right) it clearly appears also how the maximum efficiency temperature shift toward higher temperatures for smaller values of the heat-loss coefficient  $U$ . However in all cases, the optimal working temperature is found to be in the range 450–650 K. In this range several thermoelectric materials

**Figure 4.**  $\eta_{opt}$  for OC-HTPEV (black lines) and TC-HTPEV (blue lines) systems versus the total concentration,  $C_{tot}$ . Dotted, dashed and full lines refer respectively to  $U = 10, 50,$  and  $200$  W/m<sup>2</sup>K.

and alloys, such as LAST, TAGS, Zn<sub>4</sub>Sb<sub>3</sub>, and PbTe, have been reported to show  $ZT \geq 1$ .<sup>16–18</sup>

From the comparison of the absolute values of the efficiencies in the two systems one may also conclude that the TC-HTPEV system is expected to perform better than the OC-HTPEV one. The reason for this result comes from the fact that  $\eta_{opt}$  is found to be much higher for the TC-HTPEV (Fig. 4). However this efficiency gap could be covered considering larger  $C_{opt}$  for the OC-HTPEV system.

Figure 5 reports instead the total efficiencies of the two HTEPV systems versus the dissipater heat-loss coefficient  $U$ . In both cases the optimal  $C_{tot}$  values were found. For the OC-HTPEV device three  $C_{opt}$  values were considered.

**Figure 3.** Total efficiencies for OC-HTPEV (black lines) and TC-HTPEV (blue lines) systems versus total concentration  $C_{tot}$  (left), and versus  $T_h$  (right). Dotted, dashed and full lines are respectively the case of  $U = 10, 50$  and  $200$  W/m<sup>2</sup>K.

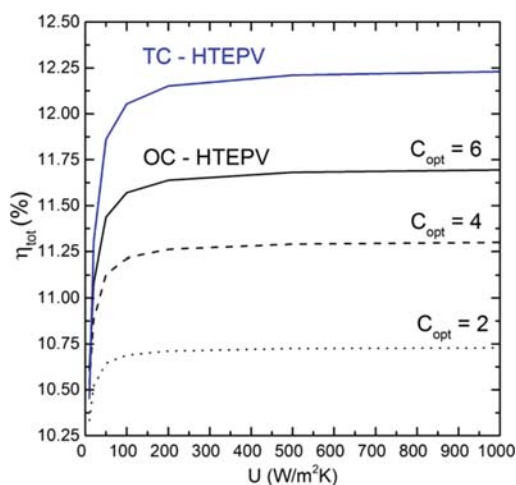


**Figure 5.** Total efficiencies for OC-HTEPV (black lines) and TC-HTEPV (blue line) systems versus the dissipater heat-loss coefficient  $U$ . Dotted, dashed and full lines refer respectively to  $C_{opt} = 2, 4,$  and  $6$ .

Notably, all curves show a plateau for  $U$  values above  $200 \text{ W/m}^2\text{K}$ , clearly indicating that low cost heat dissipater are sufficient to reach optimal efficiency improvements.

In particular, efficiencies of about 12.2% were computed for the TC-HTEPV system, while for the OC-HTEPV system efficiencies around 10.7%, 11.3% and 11.7% were estimated, respectively for  $C_{opt} = 2, 4,$  and  $6$ .

## 5. CONCLUSIONS

For both solutions the model returns conversion efficiencies larger than that of the CZTS solar cell alone when suitable total and/or optical concentration are used along with a cooling system. Specifically, increases of  $\approx 34$  and  $29\%$  are predicted respectively for the TC-HTEPV and the OC-HTEPV systems.

The maximum efficiencies and optimum total (thermal) concentrations were practically constant as a function of heatsink thermal coefficient  $U$  for values higher than  $200 \text{ W/m}^2\text{K}$ . Therefore from a practical point of view an air cooled system appears to be sufficient in all cases.

From the comparison of the two HTEPV systems proposed, it is not immediate to choose which one is the best solution. In fact, taking only the conversion efficiency as the comparison parameter, it results that the TC-HTEPV system can perform better than the OC-HTEPV one. However the latter is advantaged by the smaller quantity of active thermoelectric material it needs, and the smaller areas which must be covered by cooling devices. This should lower the costs compared to the first solution. Therefore a more detailed comparison between pros and cons (including a cost evaluation of the two systems) is needed to reach a final conclusion about the best solution to be pursued in the future.

Finally it is worth to consider that from a technological point of view the need of a sub-gap absorber for the TC-HTEPV and especially of a transparent back contact for the OC-HTEPV are key elements for the actual feasibility of these systems. Therefore a research effort on back-contact engineering is crucially recommended for the development of these promising hybrid solar solutions.

## APPENDIX: EQUIVALENT EMISSIVITY OF A TWO-SURFACE ENCLOSURE AND THE CASE OF A CPC

In general, the heat transferred by radiation in a two-surface enclosure from a surface of area  $A_1$  to that of area  $A_2$ , with temperatures respectively  $T_1$  and  $T_2$ , can be expressed by<sup>15</sup>

$$q_{1 \rightarrow 2} = \frac{\sigma(T_1^4 - T_2^4)}{(1 - \varepsilon_1)/A_1 \varepsilon_1 + 1/(F_{1 \rightarrow 2} A_1) + (1 - \varepsilon_2)/A_2 \varepsilon_2} \quad (\text{A1})$$

where  $F_{1 \rightarrow 2}$  is the View Factor between the two surfaces.<sup>15</sup> In particular, for two very large (infinite) and parallel facing plane surfaces, being  $F_{1 \rightarrow 2} = 1$  and  $A_1 = A_2$  an equivalent emissivity can be introduced, which reduces to an expression similar to the Eq. (20)<sup>15</sup> and permits to use Stefan-Boltzmann type expression for net power exchanged.

However, as shown by Rabl,<sup>8</sup> to correctly describe the heat radiation transfer between two surfaces through specular passages, as is the case a CPC, the useful concept of Exchange View Factors must be introduced instead of the View Factors: in order to take into account the effect of a non-perfectly specular surface to the heat transfer. In any case, we note that from the point of view of heat transfer the CPC case admits a very useful approximation assuming the mirror as perfectly reflective. This is equivalent to neglect at first the absorbed heat of the CPC, assuming that it has no other effect on heat transfer than reflecting the radiation virtually modifying the geometry. In this case, the use of a fictitious View Factor can be preserved. In particular, by construction in a CPC all the radiation hemispherically emitted by the absorber intercepts the front closure within acceptance angle,<sup>7</sup> and then a relation similar to the Eq. (A1) can be used with the View Factor between absorber and front surface equal to one. Equation (18)<sup>15</sup> is then easily obtained in this approximation remembering that  $C_{opt} = S/A$ .

## References and Notes

1. X. Song, X. Ji, M. Li, W. Lin, X. Luo, and H. Zhang, *Int. J. Photoenergy* 2014, 613173 (2014).
2. T. Fukano, S. Tajima, T. Ito, W. Wang, M. T. Winkler, O. Gunawan, T. Gokmen, T. K. Todorov, Y. Zhu, and D. B. Mitzi, *Appl. Phys. Express* 4, 062301 (2013).
3. T.-J. Hsueh, J.-M. Shieh, and Y.-M. Yeh, *Prog. Photovoltaics Res. Appl.* 23, 507 (2015).
4. B. Lorenzi, M. Acciarri, and D. Narducci, *J. Mater. Res.* 30, 2663 (2015).

5. B. Lorenzi, M. Acciarri, and D. Narducci, *J. Electron. Mater.* 44, 1809 (2015).
6. O. Dupré, R. Vaillon, and M. A. Green, *Sol. Energy Mater. Sol. Cells* 140, 92 (2015).
7. R. Winston and H. Hinterberger, *Sol. Energy* 16, 89 (1974).
8. A. Rabl, *Sol. Energy* 18, 497 (1976).
9. D. Kraemer, B. Poudel, H.-P. Feng, J. C. Caylor, B. Yu, X. Yan, Y. Ma, X. Wang, D. Wang, A. Muto, K. McEnaney, M. Chiesa, Z. Ren, and G. Chen, *Nat. Mater.* 10, 422 (2011).
10. G. Chen, *J. Appl. Phys.* 109, 104908 (2011).
11. K.-T. Park, S.-M. Shin, A. S. Tazebay, H.-D. Um, J.-Y. Jung, S.-W. Jee, M.-W. Oh, S.-D. Park, B. Yoo, C. Yu, and J.-H. Lee, *Sci. Rep.* 3, 422 (2013).
12. M. A. Green, K. Emery, Y. Hishikawa, W. Warta, and E. D. Dunlop, *Prog. Photovoltaics Res. Appl.* 23, 805 (2015).
13. P. Lin, L. Lin, J. Yu, S. Cheng, P. Lu, and Q. Zheng, *J. Appl. Sci. Eng.* 17, 383 (2014).
14. F. Kreith, *The CRC Handbook of Thermal Engineering*, Springer Science and Business Media, Berlin, Germany (2000).
15. T. L. Bergman, A. S. Lavine, F. P. Incropera, and D. P. DeWitt, *Introduction to Heat Transfer*, Wiley, New York, US (2011).
16. J. R. Sootsman, D. Y. Chung, and M. G. Kanatzidis, *Angew. Chemie -Int. Ed.* 48, 8616 (2009).
17. T. M. Tritt and M. A. Subramanian, *MRS Bull.* 31, 188 (2006).
18. G. J. Snyder and E. S. Toberer, *Nat. Mater.* 7, 105 (2008).

Received: 14 March 2016. Accepted: 26 May 2016.